Journal of Magnetic Resonance **139,** 422–429 (1999)
Article ID jmre.1999.1807, available online at http://www.idealibrary.com on IDEAL®

Electrically Detected Magnetic Resonance Signal Intensity at Resonant Frequencies from 300 to 900 MHz in a Constant Microwave Field

Toshiyuki Sato,* Hidekatsu Yokoyama,†,[1] Hiroaki Ohya,†,‡ and Hitoshi Kamada†

*Yamagata Research Institute of Technology, Yamagata 990-2473, Japan; †Institute for Life Support Technology, Yamagata Technopolis Foundation, Yamagata 990-2473, Japan; and ‡Graduate School of Engineering, Yamagata University, Yonezawa 992-8510, Japan

Received February 8, 1999; revised April 27, 1999

A method for electrically detected magnetic resonance (EDMR) measurement at different ESR frequencies under a constant alternating magnetic field has been established wherein the accurate relationship between EDMR signal intensity (from a photoexcited silicon crystal and a silicon diode) and a resonant frequency of 300 to 900 MHz (UHF band) was systematically clarified. EDMR signal intensity from a photoexcited silicon crystal against a resonant frequency fitted the curve of $y = a(1 - e^{-bx})$ well, which approached a constant value at higher frequencies. The increase in the EDMR signal intensity from the silicon diode at higher resonant frequencies was smaller than that from the photoexcited silicon crystal. The difference can be explained by the influence of the skin effect; i.e., the microwaves do not penetrate deep into a highly conductive sample at higher frequencies. EDMR signal intensities of samples vs microwave power were measured at 890 MHz. The EDMR signal intensity from the silicon diode continued to increase as the microwave power was increased, while the signal intensity from the photoexcited silicon crystal saturated within the range. The difference can be similarly explained: due to the skin effect, the microwaves gradually penetrate into the silicon diode as the power increases, so that even when saturation has been reached outside, the microwave field inside the diode does not reach the saturation level. © 1999 Academic Press

Key Words: **EDMR; ESR; single-turn coil; UHF; resonant frequency.**

1. INTRODUCTION

Electrically detected magnetic resonance (EDMR) is a method for detecting ESR by observing electrical characteristics, such as changes in conductivity. The technique enhances sensitivity compared to the standard ESR, and it is particularly useful for investigating paramagnetic centers that control the performance of semiconductor devices.

The first EDMR experiment was performed by Lepine, who observed a decrease in the photoconductivity of photoexcited silicon under ESR conditions (*1*). Later, EDMR was also observed in diodes where an increase in forward bias current was detected (*2*). The change in this electrical property was due to a change in the recombination rate of conduction electrons and holes under ESR conditions. On early EDMR models, it was thought that the capture of conduction electrons by a recombination center depended on their relative spin orientations (*1*). Here the externally applied magnetic field polarized the electrons and two electrons in the same spin state could not occupy the same defect site. According to this model, the maximum relative change in the electrical property was estimated to be about 10^{-6} under standard *X*-band ESR conditions at room temperature, where the electrons and holes were always considered to be in thermal equilibrium. However, this value was two orders of magnitude smaller than that obtained experimentally (*3*).

Kaplan, Solomon, and Mott proposed a modified model (KSM model) in which electrons and holes are assumed to form triplets and singlets of localized pairs (*4*). The electron–hole pair can either recombine or dissociate but cannot recombine with other electrons and holes. It was assumed that the electron–hole pair recombined before spin relaxation could occur. Because the pair in a singlet state is allowed to recombine and the pair in a triplet state is not, most singlet states will quickly recombine, leaving the system in a triplet-rich state. When a microwave is irradiated under ESR conditions, some triplet pairs are converted into singlet pairs. Thus recombination occurred so efficiently under ESR conditions that the enhanced change in electrical properties was observed.

L'vov *et al.* have proposed a quantum theory of spin-dependent recombination via the pair state instead of the pair distribution function used in the KSM model (*5*). Rong *et al.* have proposed that the electron–hole pair in the KSM model should consist of a hole and an electron trapped on the same site in an excited state (*6*). The expressions proposed for the EDMR signal vs microwave power were shown to be in good agreement with the experimental results.

The pair model also predicts that the relation between resonant frequency and EDMR signal intensity is very different from that of the conventional ESR phenomenon. Solomon observed EDMR signals from a photoexcited amorphous silicon film at ESR frequencies of 1.9 and 9.5 GHz (*7*). It was reported that a relative change in photoconductivity close to 10^{-3} was observed at both frequencies. Vranch *et al.* confirmed

[1] To whom correspondence should be addressed.

1090-7807/99 $30.00

that the change in current through an irradiated MOSFET diode area induced by ESR was of the order of 10^{-4} over a range of 7–12 GHz. They also measured the change to be in the same order at 440 MHz (*8*).

Brandt *et al.* presented a comparison of the EDMR signal intensities observed in amorphous hydrogenated silicon (a-Si:H) at 434 MHz and 9 and 34 GHz in a wide range of microwave fields (*9*). In their report, the error observed was larger than the changes in conductivity at these frequencies in the same microwave field. On the other hand, Barabanov *et al.* measured EDMR from 2 to 10 MHz (*10*). They reported that EDMR signal intensity against the resonant frequency was a good fit to the theoretical curve $ax^2 + b$ (*5*). Thus it is believed that EDMR signal intensity is constant at higher resonant frequencies and decreases with the resonant frequency in the lower bands.

If it were possible to observe EDMR at low frequencies (e.g., in the UHF band) without sacrificing sensitivity, a number of advantages would ensue. Because the wavelength of microwaves at low frequencies increases, a large resonator can be constructed. In this case, a whole device or a semiconductor wafer can be placed in the resonator. The influence of wires connected to the sample for detecting changes in electrical properties or encapsulation of a semiconductor device, which would easily disturb the resonant mode in a small resonator (e.g., a conventional *X*-band resonator), is reduced. The skin depth is also greater at lower frequencies: thus a highly doped semiconductor that has high conductivity can be efficiently measured.

Experiments have been conducted to observe EDMR at low frequencies (*8–10*). However, no systematic experiments have been reported in which an accurate relationship between the EDMR signal intensity and ESR frequency within the UHF band is established. In our experiment, EDMR was observed within the UHF band, where the wavelength is 0.1 to 1 m in vacuum. In this frequency band, a sufficient sample space is available.

It is necessary to control the alternating magnetic field, B_1, accurately at various frequencies to define the characteristics of EDMR signal intensity vs ESR frequency. A single-turn coil was used for this purpose (*11*). When the diameter of a single-turn coil is small relative to the wavelength of the microwaves, the magnetic field in the coil can be easily estimated by measuring the applied forward microwave power. It might be possible to manufacture plural resonators that resonate at different frequencies. When a high-*Q* microwave resonator is used, it is possible to irradiate a sample with microwave power efficiently. However, it is difficult to control the B_1 field constant when the *Q* values and filling factors are different. Furthermore, the B_1 field strength readily fluctuates with a small change in tuning conditions.

In this study, the EDMR of a photoexcited silicon crystal and a diode was measured at 300 to 900 MHz. The experiment employed a single-turn coil to obtain the precise relationship between the EDMR signal intensity and the ESR frequency in a constant microwave field. To examine the difference in EDMR properties between a photoexcited silicon crystal and a silicon diode, the dependence of EDMR signal intensity on the microwave power was measured at 890 MHz.

2. EXPERIMENTAL METHOD

2.1. Magnet and Microwave Unit

For the ESR instrument, a commercially available resistive magnet (modified RE3X, JEOL, Japan) was used as the main magnet. The magnetic field was swept by using a pair of field scan coils (Yonezawa Electric Wire, Japan). The microwaves were generated by an oscillator (6080A, Giga-Tronics, San Ramon; frequency range, 10 kHz to 1056 MHz). The microwave power was amplified by a power amplifier (A1000-1050, R & K, Japan; gain, 46 dB; output impedance, 50 Ω; bandwidth, 200 MHz to 1 GHz; maximum power, 50 W).

To measure EDMR signal intensity vs resonant frequency, a single-turn coil was used. Power was applied to the single-turn coil through a −3-dB attenuator (SA-51, Sanken, Japan; bandwidth, DC to 4 GHz; maximum power, 5 W) and a directional coupler (HP778D, Hewlett–Packard, Palo Alto, CA; bandwidth, 100 MHz to 2 GHz; coupling coefficient, −20 dB). The single-turn coil (8 mm in diameter) made of copper wire (1 mm in diameter) was soldered to a semirigid coaxial cable (3.6 mm in diameter), which had a characteristic impedance of 50 Ω. The attenuator was used to improve the VSWR output properties of the power amplifier and to protect the amplifier from the reflected microwaves from the single-turn coil. The directional coupler was employed so that the forward microwave power could be observed. A power meter (HP437B, Hewlett–Packard; bandwidth, 0.1 to 18 GHz) measured the microwave power at the directional coupler's reference port.

A bridged loop–gap resonator (BLGR) was used to measure the dependence of the EDMR signal on the microwave power (*12–15*). It is necessary to apply a homogeneous B_1 field to the samples for this measurement. In this case, the diameter of the single-turn coil must be several times larger than the whole sample size. This necessitates a very high irradiating power to provide a sufficient B_1 field for the sample when such a large single-turn coil is used. When a high-*Q* resonator such as the BLGR is used, it is possible to apply a B_1 field to the sample more efficiently. Although it is difficult to control the B_1 field in the resonator precisely as noted above, it is possible to compare the microwave power property of the two samples using a single resonator at a microwave frequency. The B_1 field in the resonator can be estimated from the *Q* value, dimensions of the resonator, and applied microwave power. The B_1 field strength is given by

$$B_1 = \frac{\mu_0}{2q} \cdot \sqrt{\frac{Q_L W}{\omega L}}, \qquad [1]$$

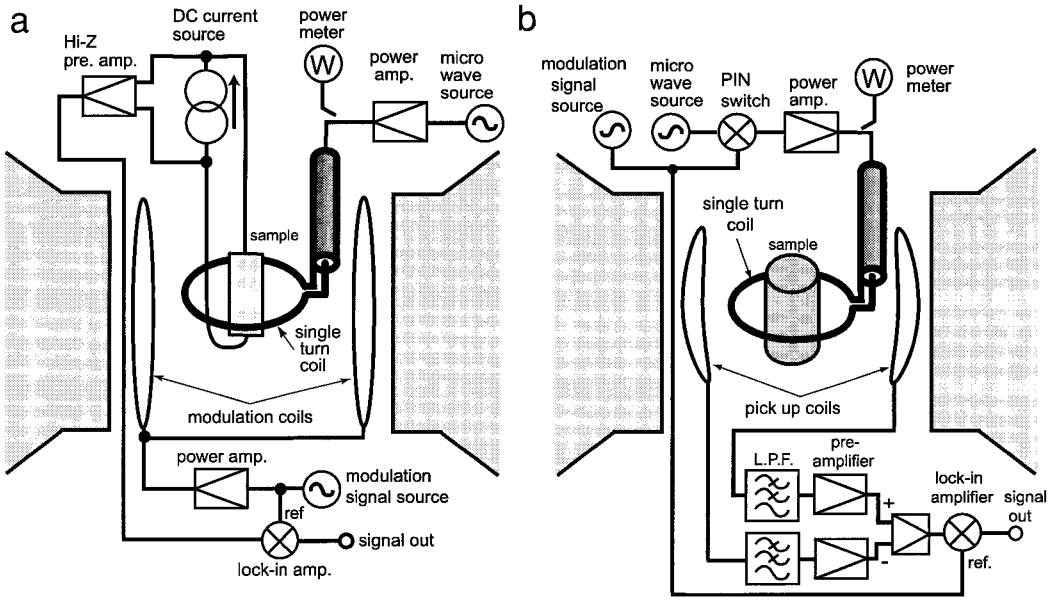

FIG. 1. Block diagram of (a) EDMR and (b) LODESR spectrometers.

where μ_0 is the permittivity of free space; q, the radius of the BLGR; Q_L, the loaded Q value of the resonator; W, the applied microwave power; ω, the angular velocity of the microwaves; and L, the inductance of the loop conductor. The inductance is given by

$$L \approx \frac{\mu_0 \pi q^2}{p + q - 0.02(q^2/p)}, \qquad [2]$$

where p is the axial length of the BLGR. The BLGR was a four-gap type, with interior and exterior bridge shields. The center frequency was 890 MHz. The bridged shields were located at the gaps via Teflon spacers that were 0.5 mm thick. The radius of the BLGR, q, was 22 mm and the axial length, p, was 10 mm. A magnetic loop coupling was used, where the coupling could be adjusted by moving the loop along the axis. Because the diameter was large relative to the samples, a homogeneous magnetic field was applied. The loaded Q values for both samples were the same ($Q_L = 510$).

2.2. EDMR Setup

A block diagram of the EDMR spectrometer is shown in Fig. 1a. A photoexcited silicon crystal and a silicon diode were used as samples, which were biased at a constant current of 10 μA supplied by a DC current source (constructed in our laboratory).

The change in voltage across the sample was detected by a high input impedance preamplifier (constructed in our laboratory; input impedance, 9×10^{11} Ω and 1 nF in parallel; gain, 40dB; bandwidth, 2 Hz to 5 kHz) followed by a lock-in amplifier (Model 5210, PARC, Princeton, NJ; bandwidth, 0.5 Hz to 120 kHz). The magnetic field was modulated at 320 Hz for lock-in detection by a pair of modulation coils. When the magnetic field was swept by using the pair of field scan coils at a constant microwave frequency, a differential EDMR spectrum was obtained.

In the measurement of a photoexcited silicon crystal, a decrease in photoconductivity under ESR conditions was obtained as the EDMR signal. An (100) oriented slice of a rectangular n-type silicon crystal (width, 2 mm; length, 15 mm; thickness, 0.5 mm; resistance, 5 kΩ-cm) was used. Electrodes were constructed at both sides of a rectangular plate located in an open area (15 mm in length). Chromium was deposited to a thickness of 400 Å onto the surface of a polished silicon plate to produce the electrodes with ohmic contact. Gold was deposited onto the chromium layer to a thickness of 2000 Å. Copper wires (0.26 mm in diameter) were soldered to the electrodes. An electric light bulb (1 W) was used to illuminate the sample, which was placed at the center of the single-turn coil. A schematic setup of the sample and the single-turn coil is shown in Fig. 2a.

Another sample was a diode (1N4007, a pn+ type silicon diode) where an increase in the recombination current under ESR conditions was observed as the EDMR signal. Because the diode was forward biased at a constant current, a decrease in voltage was measured in this experiment. The schematic setup of the sample diode is shown in Fig. 2b. The diode was placed at the center of a single-turn coil. The diode device was set so that it was perpendicular to the B_1 field and the electrodes did not disturb the field penetration. The lead wires attached to the diode were cut. The encapsulation was scraped to shorten the whole length of the device and reduce the electrical coupling between the diode and the single-turn coil.

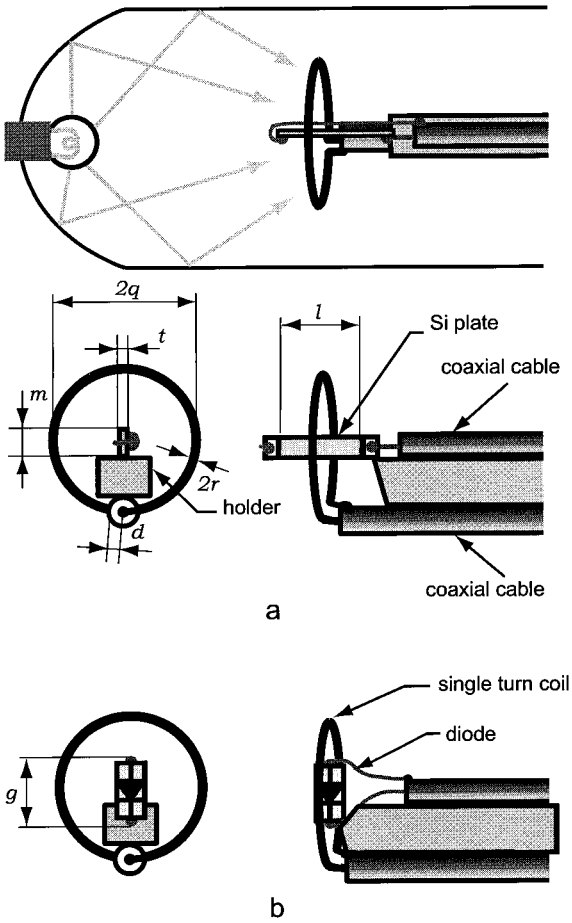

FIG. 2. Schematic representation showing the positions of a single-turn coil and a sample for EDMR measurement. The single-turn coil was made of copper wire (r, 0.5 mm radius). The radius of the coil, q, was 4 mm. The coil was soldered to a semirigid coaxial cable (3.6 mm in outer diameter) that had a 50-Ω characteristic impedance. The width of the gap that interrupts the circle of the single turn coil, d, was 1.8 mm. The length, l, width, m, and thickness, t, of the silicon crystal plate shown in (a) were 15, 2, and 0.5 mm, respectively. The lead wires of the diode shown in (b) were cut. The encapsulation was scraped to shorten the whole length of the device to reduce the electrical coupling between the diode and the single-turn coil. The length of the diode, including electrodes, g, was 4 mm. Both samples were soldered to a semirigid coaxial cable (2 mm in diameter) via copper wires (0.26 mm in diameter).

To determine the resonant frequency characteristics, measurements were made at 300, 400, 500, 600, 700, 800, and 900 MHz, using the single-turn coil. The microwave power characteristics were measured in a B_1 field of 28 to 98 μT at 890 MHz using the BLGR. Both measurements were performed at room temperature (20°C). The instrumentation was controlled by a personal computer (PC9821Xa13, NEC, Japan); and the spectral data were collected via an A/D converter (ADJ98, Canopus Co. Ltd., Japan), also using a personal computer.

2.3. Controlling the B_1 Field at Different Frequencies

When the radius of a single-turn coil is small relative to the length of the microwaves, a constant current in the coil can be assumed. When the output impedance of the power amplifier and the characteristic impedance of the attached coaxial cable are the same and have no imaginary component, they can be regarded as a voltage source that has an internal impedance of Z_0. When a single-turn coil is driven by the signal source at microwave power, W, the strength of the magnetic field, B_1, at the center of the coil is calculated by

$$B_1 = \left(1 - \frac{\sin^{-1}(d/2q)}{\pi}\right) \cdot \frac{\mu_0 \sqrt{WZ_0}}{q|R + j\omega L + Z_0|}, \qquad [3]$$

where L is the inductance of the coil; R, a loss component that is expressed as the resistance of the coil; q, the radius of the coil; and d, the width of the gap that interrupts the circle (*11*).

In accordance with Eq.[3], a constant B_1 field can be applied by controlling the microwave power at the frequencies given above. The equation shows that maximum power must be applied at 900 MHz, the highest frequency used in this experiment. The microwave power was set at 2 W for the EDMR measurement at 900 MHz. Under this condition, the B_1 field strength at the center of the single turn coil was 39.2 μT.

2.4. Confirmation of the B_1 Field Control System

Because it is difficult to measure the B_1 field strength directly in a single-turn coil, longitudinally detected ESR (LODESR) (*16–18*) was employed for this purpose. In LODESR measurements, the microwaves are pulse-modulated under the ESR condition and the longitudinal change in magnetization is detected by pickup coils. When the detection frequency of LODESR (i.e., the modulation frequency) is fixed, the sensitivity of a LODESR detector is constant at different resonant frequencies. LODESR signal intensities were measured by using the single-turn coil to validate the B_1 field control system at the magnetic resonant frequencies.

A schematic diagram of the LODESR components is shown in Fig. 1b. A pair of saddle-type pickup coils (*18*), each constructed from 15 turns of copper wire (0.3 mm in diameter), were used. The outer diameter of a coil was 30 mm. These coils were glued onto a cylindrical quartz glass tube (39 mm in outer diameter). The signals from the right and left pickup coils, which were characterized by reverse polarity, were amplified separately by two preamplifiers (SA-230F5, NF Electronic Instruments, Japan; gain, 46 dB; bandwidth, 1 kHz to 100 MHz; noise figure, 0.6 dB). The difference in outputs from the preamplifiers was amplified by a differential amplifier (5305, NF Electronic Instruments; bandwidth, DC to 10 MHz) to reduce common mode noise. The microwaves were on/off modulated, using a function generator (AFG320, Sony-Techtronix, Japan; maximum frequency, 16 MHz) and a pin switch (ZYSWA, Mini circuit, New York, NY; bandwidth, DC to 5 GHz; switching time, 5 ns). The modulation frequency was detected by a lock-in amplifier (5202, PARC, Princeton, NJ; bandwidth, 0.1 to 50 MHz).

To obtain sufficient signal strength, 90 mg of 1,1-diphenyl-2-picrylhydrazyl (DPPH) powder was used. The modulation frequency was 1.35 MHz, with an on/off ratio of 1:1. The induced voltage in the pickup coils increases in proportion to the change in the modulation frequency. However, when the modulation frequency increases close to the order of T_1^{-1} of the sample, the signal intensity will decrease. We confirmed that no saturation effect occurred with this sample at the modulation frequency. The average microwave power for the LODESR measurements was set to 2 W at 900 MHz. Under this condition, the B_1 field strength at the center of the single-turn coil was 55.4 μT for the "on" period of the on/off modulation.

3. RESULTS AND DISCUSSION

LODESR spectra of DPPH at 300, 500, 700, and 900 MHz are shown in Fig. 3a. The absorption linewidth as well as the lineshape did not change at these frequencies. The signal intensities obtained experimentally at 300 to 900 MHz are shown in Fig. 4. The signal intensity increased linearly when the resonant frequency increased. The correlation coefficient for the linear approximation was 0.991. Theoretically, the LODESR signal intensities of an organic free radical are proportional to the resonant frequency. The difference in unpaired electron spin numbers at higher and lower levels of Zeeman splitting is proportional to the splitting width at room temperature and the resonant frequencies. There was good agreement between the theory and the results, so this measuring system (i.e., B_1 field control system) was proven to be properly designed and constructed. The worst signal-to-noise ratio (SNR) across the LODESR spectrum occurred at 300 MHz: it was 60.

The main factor contributing to the errors in this measuring system appeared to be the characteristics of the directional coupler. The parameters of the directional coupler under these experimental conditions were calibrated by using a network analyzer (HP8720B, Hewlett–Packard; bandwidth, 130 MHz to 20 GHz). However, it was difficult to reduce the error due to the directional coupler below other error factors such as the SNR over the spectrum because the single-turn coil was an undesirable load that had a very large VSWR. The maximum error in this measurement was 5%.

EDMR spectra of a photoexcited silicon crystal at 300, 500, 700, and 900 MHz are shown in Fig. 3b. The lineshapes did not change at these frequencies. The signal intensities obtained experimentally at 300 to 900 MHz are shown in Fig. 5. The EDMR signal intensity increased only sublinearly when the resonant frequency was increased (the increase in EDMR signal intensity with the increase in ESR frequency was smaller than that of a linear relationship). The theoretical curve of $y = ax^2 + b$ (*5*) did not fit well to our results (Fig. 5, dotted line, correlation coefficient = 0.972). In our experiment $B_0 \gg B_1$ (where B_0 is the static magnetic field) so the b in the theoretical

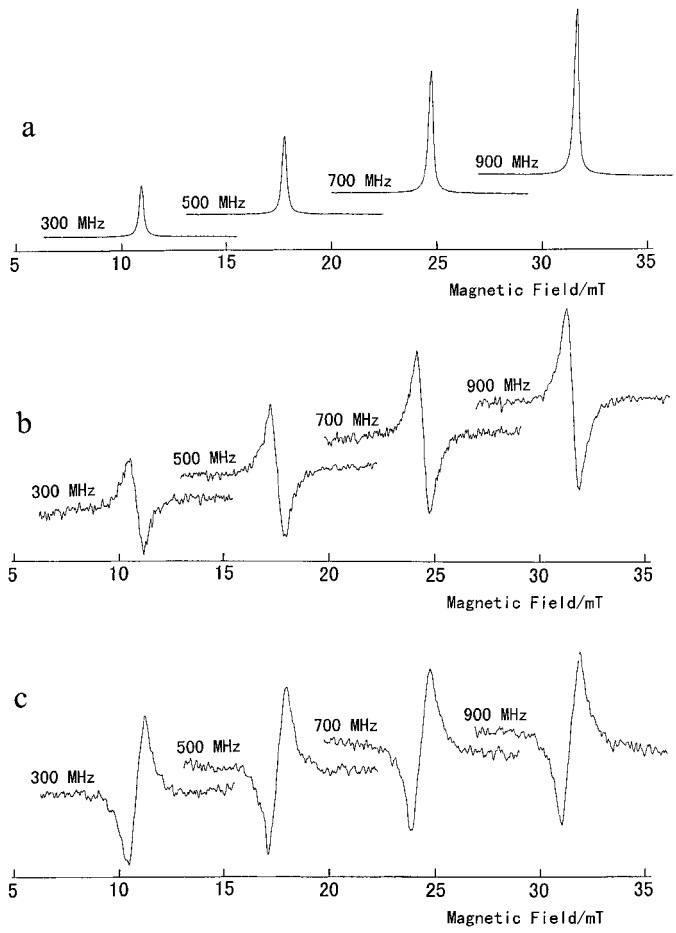

FIG. 3. (a) LODESR spectra of DPPH, (b) EDMR spectra of photoexcited silicon crystal, and (c) EDMR spectra of a silicon diode at 300, 500, 700, and 900 MHz. The sweep time was 2 s and the sweep width, 15 mT. In this figure, 10 mT around the absorption signal was extracted. The time constants were 0.001 and 0.003 s for the LODESR and EDMR measurements, respectively. The LODESR spectra were averages of 16 sweeps. EDMR spectra were averages of 64 sweeps of the photoexcited silicon crystal and 256 sweeps of the diode.

equation must be very small. However, the value of b obtained here was fairly large.

We introduced a fitting curve, $y = a(1 - e^{-bx})$, where the signal intensity approaches a constant value at higher frequencies, which is consistent with the experimental results obtained at the higher resonant frequencies (*7–9*). The curve also represents our experimental results, in which the signal intensity approaches zero at the lower resonant frequency. The signal intensities fitted the curve well (Fig. 5, solid line, correlation coefficient = 0.996). The resonant frequency at which the signal intensity reaches half value (i.e., $a/2$) was 444 MHz for this curve. A study on the physical significance of this fitting is now underway, but it was consistent with the general concept that the signal intensity is constant in a high frequency range and a signal decreases with the ESR frequency over a low frequency range.

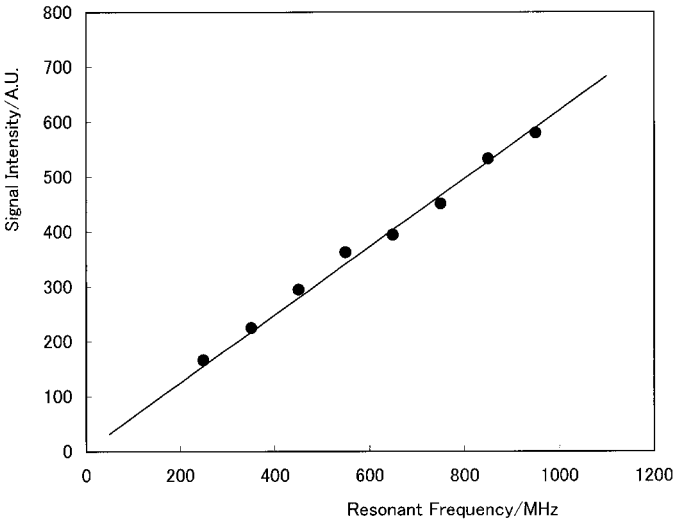

FIG. 4. LODESR signal intensities of DPPH from 300 to 900 MHz. Solid circles show experimental results. The solid line shows the fit of $y = ax$ (correlation coefficient = 0.991).

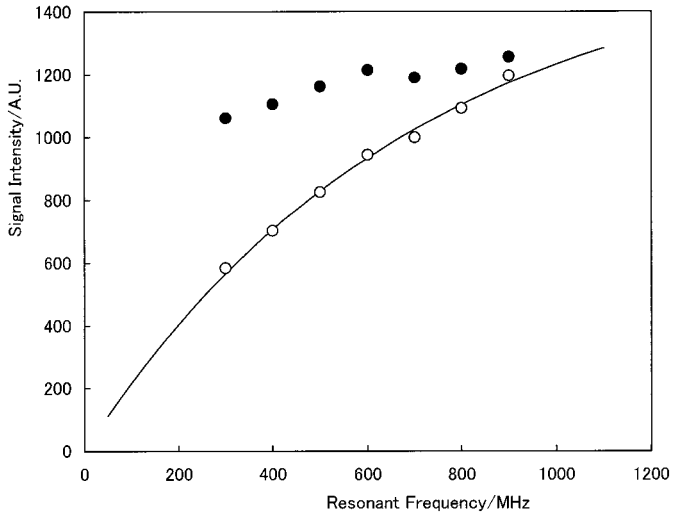

FIG. 6. EDMR signal intensities of a diode from 300 to 900 MHz. Solid circles show experimental results. Open circles are corrected results. The curve (solid line) shows the fit of $y = a(1 - e^{-bx})$ for the corrected results, where $b = 1.44 \times 10^{-9}$ (correlation coefficient = 0.997).

EDMR spectra of a silicon diode, 1N4007, at 300, 500, 700, and 900 MHz are shown in Fig. 3c. Because the signals from the diode were detected as an increase in conductivity under the ESR condition, the spectra were the reverse of those for the photoexcited silicon crystal, where a decrease in conductivity was detected. The lineshape was the same at each frequency. The signal intensities obtained experimentally at 300 to 900 MHz are shown in Fig. 6. The increase in signal intensity from the diode as the resonant frequency increased was less than that of the photoexcited silicon. This can be explained by the fact that the microwaves did not penetrate the sample sufficiently at the higher frequencies because of the high conductivity of the diode material. The skin depth of the sample can be expressed as

$$\delta = \sqrt{\frac{2}{\omega\mu\sigma}}, \qquad [4]$$

where μ is the permittivity of the sample, and σ, the conductivity of the sample. The averaged conductivity of the photoexcited silicon was 0.11 S/m. Its skin depth at 900 MHz, the maximum frequency in this experiment, was calculated to be 51 mm. This value was large relative to the width or thickness of the sample.

The conductivity of the diode material was very high due to the high concentration of the doped carrier. The equivalent series resistance of the diode was determined to be 0.05 Ω from a current–voltage characteristic. Since the chip size of the diode was measured to be $1 \times 1 \times 0.3$ mm, the average conductivity and the skin depth of the diode substrate at 300 MHz, the minimum frequency in this experiment, were calculated to be 7×10^4 S/m and 0.1 mm, respectively.

The B_1 field distribution in the diode is complicated but a rough estimation can be made by using a transmission line model. A semiconductor between and attached to two electrodes can be assumed to be a parallel plate transmission line (see Fig. 7). The microwaves were irradiated from both sides of the transmission line. The magnetic field distribution in the transmission line can be expressed by

$$B_1(z) = \frac{B_{1i}}{1 + \exp\left(\dfrac{-l}{\delta}\right)} \left\{ \exp\left(\frac{-z}{\delta}\right) + \exp\left(\frac{z - l}{\delta}\right) \right\}, \qquad [5]$$

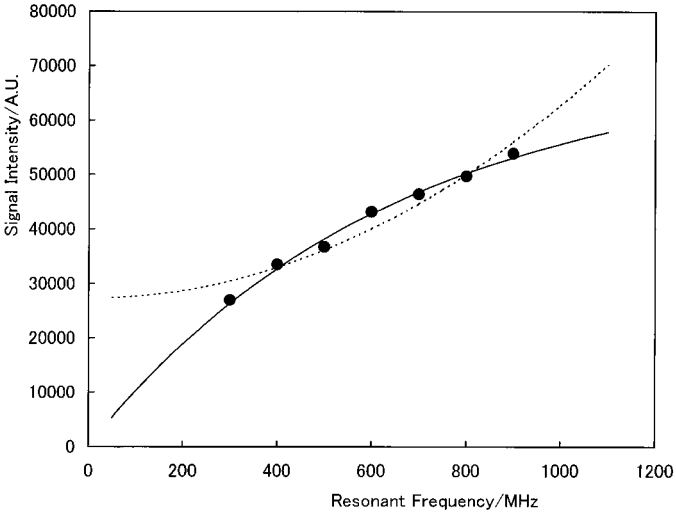

FIG. 5. EDMR signal intensities of a photoexcited silicon crystal from 300 to 900 MHz. Solid circles show experimental results. The curve fits $y = a(1 - e^{-bx})$, where $b = 1.56 \times 10^{-9}$, which is drawn as a solid line (correlation coefficient = 0.996). The dotted line shows the fit of $y = ax^2 + b$ (correlation coefficient = 0.972).

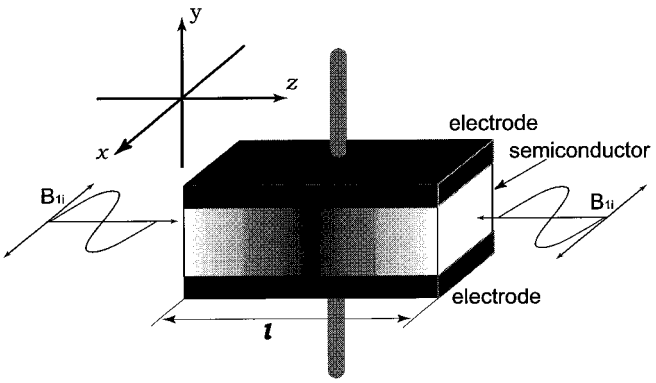

FIG. 7. Parallel plate transmission line model for estimating the magnetic field distribution in the diode chip. The microwaves are irradiated from both sides of the transmission line. The line length is 1 mm; the distance between plates, 0.3 mm; and the width of a plate, 1 mm.

where l is the length of the transmission line and B_{1i}, the magnetic field strength on both sides of the transmission line. The microwave phase rotation in the transmission line is negligible because the length of the line is small relative to the wavelength of the microwaves. Because the EDMR signal intensity for unsaturated microwave power is proportional to B_1^2, the signal intensity can be corrected by

$$S_{\text{corrected}} = S \cdot K = S \cdot \frac{\int_0^l B_{1i}^2 dz}{\int_0^l B_1(z)^2 dz}. \qquad [6]$$

When $l \gg \delta$, K is proportional to $1/\delta$ in accordance with Eq. [6]. The corrected signal intensities from the diode, plotted in Fig. 6, also fitted the $y = a(1 - e^{-bx})$ curve well, with a correlation coefficient of 0.997. When the fitting result is applied, the resonant frequency at which the signal intensity reaches half value (i.e., $a/2$) is estimated to be 482 MHz for the corrected signal intensity of the diode. This corresponds well to the value for the photoexcited silicon crystal (444 MHz). The measured signal intensity from the diode will decrease at higher frequencies due to a smaller skin depth. It is estimated that the EDMR signal intensity from the diode, which has a small skin depth relative to the physical size of the sample, will be a maximum at 880 MHz and will fall to half of that at 80 MHz and 6.5 GHz.

To confirm the skin effect, the microwave power properties of EDMR signal intensities from the two samples were measured at 890 MHz, using a BLGR. The results are shown in Fig. 8. The signal intensity from the diode continued to increase in a higher microwave field, while the signal intensity of the photoexcited silicon crystal was saturated within the same range. The peak-to-peak widths of the differential EDMR spectrum of the photoexcited silicon crystal and the diode were 1.1 and 1.0 mT, respectively, in a 35-μT microwave field. A slight increase in linewidth with the increase in microwave field was observed only for the diode at higher microwave field. The increase from 35 to 98 μT of microwave field was 10%. Because the linewidths of the two samples were close, the near saturation levels are expected. The difference in B_1 field characteristics for the two samples can be explained by the skin effect; i.e., even after the B_1 field around the diode exceeds the saturation level, the B_1 field deep inside the diode is not saturated and the signal intensity still continues to increase with the microwave power. Although it is possible to

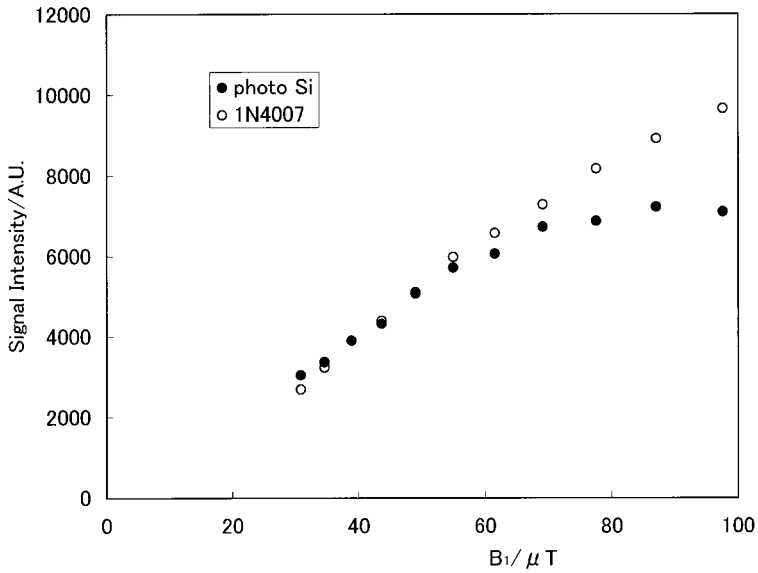

FIG. 8. EDMR signal intensities from photoexcited silicon and diode between 28 and 98 μT at 890 MHz. For both samples, bias current is 10 μA; modulation frequency, 320 Hz; scan time, 2 s; and sweep width, 15 mT. The spectra of photoexcited silicon and diode were obtained from an average of 16 and 32 sweeps, respectively.

explain that the EDMR signals of the photoexcited silicon crystal and the diode are derived from different species, causing the properties of the two samples to be different, it is more reasonable to explain the difference by citing the skin effect.

In summary, this work presents a method for EDMR measurement at different ESR frequencies under a constant B_1 field. An accurate relationship between EDMR signal intensity (from a photoexcited silicon crystal and a silicon diode) and a resonant frequency in the UHF band was elucidated. EDMR signal intensity plotted against resonant frequency fitted the curve $y = a(1 - e^{-bx})$ well, approaching a constant value at the higher frequencies. The increase in the EDMR signal intensity from a silicon diode at the higher resonant frequencies was smaller than that from the photoexcited silicon crystal. This was due to the influence of the skin effect; i.e., the microwaves did not penetrate deeply into the highly conductive sample. The difference in the microwave power properties of a photoexcited silicon crystal and the silicon diode supports this explanation.

We believe that the findings in the present study strongly support the validity of low-frequency EDMR measurements of a semiconductor, such as a whole body of silicon device in the UHF band.

ACKNOWLEDGMENTS

We thank Professor M. Ono and Dr. H. Hirata of Yamagata University and Dr. K. Fukui and Mr. H. Noda of Yamagata Technopolis Foundation for their helpful discussions, and Mr. T. Mineta of Yamagata Research Institute of Technology for his assistance in manufacturing a silicon plate with electrodes. This study was supported by the Yamagata Technopolis Foundation.

REFERENCES

1. D. Lepine, *Phys. Rev. B* **6,** 1436 (1972).
2. I. Solomon, *Solid State Commun.* **20,** 215 (1976).
3. I. Solomon, *in* "Proceedings, 11th International Conference on the Physics of Semiconductors," p. 27, Polish Scientific, Warsaw (1972).
4. D. Kaplan, I. Solomon, and N. F. Mott, *J. Phys. (Paris)* **39,** L51 (1978).
5. V. S. L'vov, L. S. Mima, and O. V. Tretyak, *Sov. Phys. JETP* **56,** 4, 897 (1982).
6. F. C. Rong, W. R. Buchwald, E. H. Poindexter, W. L. Warren, and D. J. Keeble, *Solid-State Electron.* **34,**835 (1991).
7. I. Solomon, *Bull. Magn. Reson.* **5,** 119 (1983).
8. R. L. Vranch, B. Henderson, and M. Pepper, *Appl. Phys. Lett.* **52,** 14, 1161–1163 (1987).
9. M. S. Brandt, M. W. Bayerl, N. M. Reinacher, T. Wimbauer, and M. Stutzmann, *Mater. Sci. Fourum* **258–263,** 963–968 (1997).
10. A. V. Barabanov, V. A. L'vov, and O. V. Tretyak, "23rd International Conference on the Physics of Semiconductors, 1996," Vol. 4.
11. T. Sato, H. Yokoyama, H. Ohya, and H. Kamada, *Appl. Magn. Reson.* **16,** 33–43 (1999).
12. W. N. Hardy and L. A. Whitehead, *Rev. Sci. Instrum.* **52,** 213 (1981).
13. W. Froncisz and J. S. Hyde, *J. Magn. Reson.* **47,** 515 (1982).
14. M. Ono, T. Ogata, K. Hsieh, M. Suzuki, E. Yoshida, and H. Kamada, *Chem. Lett.,* 491 (1986).
15. H. Hirata and M. Ono, *Rev. Sci. Instrum.* **67,** 73 (1996).
16. A. Colligiani, D. Leporini, M. Lucchesi, and M. Martnelli, *in* "Electron Magnetic Resonance of Disorder Systems" (N. D. Yordanov, Ed.), pp. 16–37, World Scientific, Singapore (1991).
17. I. Nicolson, F. J. L. Robb, and D. J. Lurie, *J. Magn. Reson. B* **104,** 284 (1994).
18. H. Yokoyama, T. Sato, T. Ogata, H. Ohya-Nishiguchi, and H. Kamada, *J. Magn. Reson.* **129,** 201 (1997).